Structure and Dynamics of Melittin in Lysomyristoyl Phosphatidylcholine Micelles Determined by Nuclear Magnetic Resonance

Peng Yuan,* Phyllis J. Fisher,‡ Franklyn G. Prendergast,‡ and Marvin D. Kemple*
*Department of Physics, Indiana University-Purdue University Indianapolis, Indianapolis, Indiana 46202-3273, and ‡Department of Pharmacology, Mayo Foundation, Rochester, Minnesota 55905 USA

ABSTRACT Mixed micelles of the 26-residue, lytic peptide melittin (MLT) and 1-myristoyl-2-hydroxyl-sn-glycero-3-phosphocholine (MMPC) in aqueous solution at 25°C were investigated by ^{13}C- and ^{31}P-NMR spectroscopy. $^{13}C\alpha$ chemical shifts of isotopically labeled synthetic MLT revealed that MLT in the micelle is predominantly α-helical and that the peptide secondary structure is stable from pH 4 to pH 11. Although the helical transformation of MLT as determined from NMR is evident at lipid:peptide molar ratios as low as 1:2, tryptophan fluorescence measurements demonstrate that well-defined micellar complexes do not predominate until lipid:peptide ratios exceed 30:1. ^{31}P linewidth measurements indicate that the interaction between phosphate ions in solution and cationic groups on MLT is pH dependent, and that the phosphoryl group of MMPC senses a constant charge, most likely +2, on MLT from pH 4 to pH 10. ^{13}C-NMR relaxation data, analyzed using the model-free formalism, show that the peptide backbone of MLT is partially, but not completely, immobilized in the mixed micelles. Specifically, order parameters (S^2) of Cα-H vectors averaged ~0.7 and were somewhat larger for residues in the N-terminal half of the molecule. The amino terminal glycine had essentially the same range of motion as the backbone carbons. Likewise, order parameters for the trp side chain were similar to those found for the peptide Cα moieties, as was verified by trp fluorescence anisotropy decay data. In contrast, the motion of the lysine side chains was less restricted, the average S^2 values for the Cϵ-H vectors being 0.19, 0.30, and 0.44 for lys-7, 21, and 23, respectively, for MLT in the mixed micelles. Values of the effective correlation time of the local motion τ_e were in the motional narrowing limit and usually longer for side-chain atoms than for those in the backbone. The dynamics were independent of pH from pH 4 to pH 9, but at pH 11 the correlation time for the rotational motion of the mixed micelles as a whole increased from 10 ns to 16 ns, and S^2 for the lys side chains increased. Overall it appears that the MLT helix lies near the surface of the micelle at low to neutral pH, but at higher pH its orientation changes, accompanied by deeper penetration of the lys side chains into the micelle interior. It is apparent, however, that the MLT-lipid interaction is not dependent on deprotonation of any of the titratable cationic groups in the peptide in the pH 4–10 range, and that there is substantial backbone and side-chain mobility in micelle-bound MLT.

INTRODUCTION

Despite extensive investigation, details of the location, orientation, and precise mechanisms of interaction of lipid-binding peptides with lipids remain unclear. A wide variety of surface interacting and surface active peptides and signal peptides have been investigated. One structural motif has predominated, namely, the amphiphilic helix, with the view that the side chains comprising the hydrophobic surface can penetrate sufficiently into the fatty acyl chain region of the lipid bilayer to stabilize the peptide-lipid complex through van der Waal's interactions with the acyl chains. Such a model carries with it clear implications regarding likely constraints on side chain dynamics, an issue of no little interest, particularly for membrane proteins whose function is modulated by membrane flexibility. Yet, interestingly, not much has been reported on the dynamics of peptides or proteins in lipid-protein complexes, one obvious problem being the overall size of the complex, which often limits the usefulness of techniques such as NMR because of the long rotational correlation times of the complexes.

Peptide-lipid mixed micelles offer an admittedly imperfect, but still extremely useful, model system for study, provided that the micelle is not too large and that one can reasonably assume some commonality in mechanism of interaction between the peptide and the micelle- or bilayer-forming lipids. We have chosen to study the dynamics of the surface active peptide melittin because, given the similarity in conformation of micellar and phospholipid-bound melittin (MLT), we believe that mixed micelles of MLT do provide a good initial model for studying peptide dynamics in peptide lipid complexes and provide at least a first approximation of how the lipid may influence peptide dynamics.

MLT, the sequence of which is given in Fig. 1, is the major component of bee venom. It has been extensively studied, beginning with the work of Habermann and colleagues (Habermann and Jentsch, 1967; Habermann, 1972) and Kreil and co-workers (Mackler and Kreil, 1977; Kreil et al., 1980). In water, MLT undergoes a monomer-tetramer aggregation (Faucon et al., 1979; Knöppel et al., 1979; Talbot et al., 1979; Lauterwein et al., 1980; Brown et al., 1980; Bello et al., 1982; Quay and Condie, 1983; Schwartz and Beschiaschvili, 1988) at high pH, at high peptide con-

Received for publication 24 July 1995 and in final form 26 January 1996.
Address reprint requests to Dr. Marvin D. Kemple, Department of Physics, Indiana University-Purdue University Indianapolis, 402 N. Blackford St., Indianapolis, IN 46202-3273. Tel.: 317-274-6906; Fax: 317-274-2393; E-mail: mkemple@indyvax.iupui.edu.

0006-3495/96/05/2223/16 $2.00

G*-I-G*-A*-V-L*-K*-V-L*-T-T-G*-L-P-A*-L*-I-S-W*-I-K*-R-K*-R-Q-Q

FIGURE 1 The melittin sequence and ^{13}C labels used in the various synthetic peptides. The residues with ^{13}C enrichment on either the α-carbon or side chain are denoted by * in the sequence. The labeled positions in the actual peptides synthesized, (i)–(v), are also shown.

(i)	$^{13}C\alpha$-G1	$^{13}C\alpha$-A4	$^{13}C\alpha$-G12	$^{13}C\varepsilon_3$-W19	
(ii)	$^{13}C\alpha$-G3	$^{13}C\alpha$-L13	$^{13}C\alpha$-A15	$^{13}C\delta_1$-W19	$^{13}C\varepsilon$-K23
(iii)	$^{13}C\alpha$-G3	$^{13}C\alpha$-L9	$^{13}C\alpha$-A15		$^{13}C\varepsilon$-K21
(iv)			$^{13}C\alpha$-L16		$^{13}C\varepsilon$-K7
(v)		$^{13}C\alpha$-L6			$^{13}C\varepsilon$-K23

centrations, and at high ionic strength (Wilcox and Eisenberg, 1992). However, at low to neutral pH and at concentrations $\leq$ 1 mM the peptide in aqueous solution is largely a random-coil monomer. The structure of tetrameric MLT in two crystal forms grown from aqueous solution with ammonium sulfate and sodium formate (Anderson et al., 1980) was determined to 2 Å resolution from x-ray diffraction analysis (Terwilliger and Eisenberg, 1982a,b). The structure was predominantly α-helical with a bend near G12. In methanolic solution, MLT was shown to be monomeric but helical by NMR (Bazzo et al., 1988), similar to the helix found in crystals (Terwilliger and Eisenberg, 1982a,b). However, in methanol a difference does exist in a hinge region between residues 11 and 12, which leads to a different angle (~160° in methanol versus ~130° in the crystal) between the two helical segments comprising residues 2–11 and 13–26, respectively. The structure of MLT bound to perdeuterated dodecylphosphocholine (DPC) micelles was also determined by 2D-NMR and distance geometry methods (Inagaki et al., 1989; Ikura et al., 1991). MLT was found to be an α-helical rod with a kink of 135 $\pm$ 15° at residues 11 and 12, with the α-helical axes approximately parallel to the lipid-water interface.

Even with the substantial effort directed at the nature of MLT-membrane interactions (for reviews, see Bernheimer and Rudy, 1986; Dempsey, 1990), how MLT causes membrane lysis is still unclear, and there is no general agreement on the nature of MLT-membrane interactions. As pointed out by Dempsey (1990), there are two main reasons for this continuing uncertainty. First, many of the biophysical techniques used to study protein structures and interactions are difficult to apply to membrane systems. Either MLT itself or the membrane system has to be modified so that the technique may be applied. Second, because most of its charges are concentrated at the C-terminus, MLT interacts with different membranes in different ways. Although it is generally accepted that MLT is helical in lipid systems (Dawson et al., 1978; Drake and Hider, 1979; Terwilliger et al., 1982; Vogel and Jähnig, 1986; Vogel, 1987; Weaver et al., 1992; Dempsey and Butler, 1992), its orientation remains controversial (Brauner et al., 1987; Dempsey, 1990; John and Jähnig, 1991; Frey and Tamm, 1991).

The dynamics of lipid-bound MLT have not been thoroughly investigated. Most of the studies to date have focused on analysis of trp side-chain mobility, determined from fluorescence anisotropy decay measurements and fluorescence lifetime distributions (Bismuto et al., 1993; Chattopadhyay and Rukmini, 1993; John and Jähnig, 1988; Vogel and Rigler, 1987; Georghiou et al., 1982). Such data have been interpreted mostly in terms of local motion of the indole ring, but inferences have been drawn regarding the overall rotational motion of the entire peptide, the most common being that lipid-bound MLT is restricted in its mobility. However, it is at best difficult and may be altogether impossible to extract information relevant to peptide chain dynamics from the fluorescence anisotropy decay of a single amino acid side chain. Instead, Weaver et al. (1992) carried out a ^{13}C-NMR dynamics study on both the trp side chain ($C\delta_1$ position) and backbone Cα of G12 of lipid micelle-bound MLT, making use of the Lipari and Szabo (1982) "model-free" approach for interpretation of the data. The motional parameters, τ_m, the overall rotational correlation time, and S^2 and τ_e (respectively, the order parameter and the effective correlation time of local motion) were obtained for both sites on the peptide. The mobility of the trp side chain was similar in the micelle and the tetramer, and was more restricted than in the monomer. Although there were insufficient data for Cα of G12 to derive motional parameters, there were indications that its motion was more limited in the micelle. Clearly even these last mentioned studies were still very limited.

In this paper we report the results of ^{13}C- and ^{31}P-NMR spectral observations of the interactions of MLT with 1-myristoyl-2-hydroxyl-sn-glycero-3-phosphocholine (MMPC) micelles, and we describe ^{13}C-NMR relaxation studies of both peptide backbone and side-chain dynamics at selected sites of MMPC micelle-bound MLT and of MMPC itself. We chose MMPC because of its basic similarity to the diacylphosphatidylcholines in terms of the zwitterionic headgroup and (albeit single) fatty acyl group (Bangham and Dawson, 1959). Additionally, its critical micelle concentration (CMC) is very low (0.07 mM; Stafford et al., 1989), and the micelles are apparently soluble to a concentration of several millimoles per liter. We also assumed that the structure of the MMPC-MLT mixed micelle does not change over a wide pH range. For the measurements, we labeled synthetic MLT with ^{13}C at α-carbon positions and at side-chain positions of several amino acids along the sequence, as shown in Fig. 1. This was done to enhance the NMR signal intensity, to facilitate resonance assignments, and, most importantly, to use these labels as probes for the structure, orientation, and dynamics of micelle-bound MLT.

Control experiments were performed to obtain the ^{13}C-NMR chemical shifts of the enriched residues for MLT in different environments. ^{13}C-NMR relaxation parameters, T_1 (the spin-lattice relaxation time), and the NOE (the steady-state nuclear Overhauser effect) of micelle-bound MLT were measured at pH values from 4 to 11 and analyzed with the "model-free" approach (Lipari and Szabo, 1982). A parallel investigation employing ^{31}P NMR was conducted on both MMPC micelles and MMPC-MLT mixed micelles. The pH dependence of chemical shifts, linewidths, and dynamics of the complexes provides insight into how pH might influence MLT-lipid interactions. In addition, fluorescence and quasi-elastic light scattering (QLS) were used to characterize the samples and to corroborate some of the dynamics measurements. The information gathered allowed the following questions to be addressed: i) What are the conformation and the orientation of the MLT molecule when bound to an MMPC micelle? ii) How accessible to solvent is MLT when bound to MMPC micelles? iii) Can we define the dynamic behavior of micelle-bound MLT?

MATERIALS AND METHODS

Materials

^{13}C-enriched amino acids were purchased from Cambridge Isotope Laboratories (Woburn, MA). MLT labeled with ^{13}C at several sites (see Fig. 1) was prepared with an amidated C-terminus by solid-phase synthesis on methylbenz-hydrilamine resin using *tert*-butyloxycarbonyl chemistries with an Applied Biosystems (Foster City, CA) model 430 peptide synthesizer or using fluorenylmethoxycarbonyl (fmoc) chemistries on 4-2′-4′-dimethoxyphenyl-fmoc-aminomethylphenoxy resin with the Applied Biosystems 430 or 431 peptide synthesizer. The resultant peptides were purified using high-pressure liquid chromatography. The synthesis was done in the Peptide Core Facility of the Mayo Foundation (Rochester, MN). MMPC (with ^{13}C at natural abundance) was purchased from Avanti Polar Lipids (Alabaster, AL) in powder form and used without further purification. MMPC micelles were prepared by sonication of ~10 ml of 1 g lipid suspension (equivalent to 214 mM) in D_2O buffered with 50 mM phosphate for 30 min at 25 ± 2°C.

NMR, fluorescence, and QLS measurements

NMR measurements were conducted at the Indiana University-Purdue University Indianapolis (IUPUI) NMR Center. ^{13}C-NMR signals were detected directly at 75.4 MHz and 125.7 MHz on Varian Unity 300 and 500 FT spectrometers (Varian Associates, Palo Alto, CA). ^{31}P-NMR signals were detected directly at 202.3 MHz on the Unity 500 FT spectrometer. The 10-mm broadband probes used with the Unity spectrometers were obtained from Cryomagnet Systems (Indianapolis, IN). External dioxane (67.37 ppm) served as a reference for the ^{13}C spectra. Proton-decoupled ^{13}C- and ^{31}P-NMR spectra were obtained using broadband noise decoupling during signal acquisition. The standard inversion recovery pulse sequence (Martin et al., 1980), $(\pi\text{-}\tau\text{-}\pi/2\text{-Acq-}t_d)_n$, was used for T_1 measurements of both ^{13}C and ^{31}P with more than 10 τ values from 0.1 to 5 times the estimated T_1. The delay time, t_d, was at least $6T_1$. Proton decoupling during acquisition, and saturation of the proton magnetization before inversion and during recovery of the ^{13}C magnetization were applied to eliminate effects from cross-relaxation and dipolar-chemical shift anisotropy (CSA) cross-correlation (Boyd et al., 1990). The influence of dipolar cross-correlation in cases where the carbon in question had two or three attached protons was minimized by deriving the T_1 values from fitting the recovery data out to approximately $3T_1$ to a three-parameter single-exponential magnetization equation (Zhu et al., 1995a). A similar procedure was followed for the carbons with a singly attached proton using data out to $5T_1$. Steady-state ^{13}C-^1H NOE measurements were made by collecting alternate scans of the ^{13}C signals with and without enhancement into different memory blocks. The NOE values were obtained from ratios of the intensities or the areas of the enhanced and equilibrium signals. Linewidths (full width at half-maximum intensity) of ^{13}C- and ^{31}P-NMR signals were either directly measured or calculated through deconvolution of the selected peak with a Lorentzian lineshape using Varian VNMR software (version 4.1). All NMR measurements were made at a sample temperature of 25.0 ± 0.5°C.

Steady-state fluorescence intensities and anisotropy measurements were conducted with either a Perkin-Elmer MPF-66 (Norwalk, CT) or an SLM 8000 (Urbana, IL) fluorimeter with excitation at 300 nm and detection at 345 nm. Time-resolved anisotropy and fluorescence lifetime measurements were made with a time-correlated photon counting instrument with excitation at 300 nm and detection at 340 nm. Quasielastic light scattering (QLS) measurements to determine the size of the micelles were made on a Malvern 4700c light-scattering instrument employing an argon ion laser as the excitation source. Included was an Autosizer 4700 controlled with software supplied by Malvern. Data were collected at a 90° scattering angle with a wavelength of 514.5 nm. All fluorescence and QLS measurements were made on samples at temperatures of 20 ± 1°C.

Lipid titration experiments

For NMR, a MLT concentration of ~1 mM with 50 mM phosphate buffer in D_2O was chosen to ensure that only monomeric MLT was present in both the aqueous phase and presumably the lipid-binding phase at pH 4 (Lauterwein et al., 1980). Lipid titration of MLT was accomplished by successive additions of aliquots of a concentrated MMPC solution (214 mM). After each addition of MMPC, the sample was briefly agitated on a vertex mixer. The binding of MMPC lipid to each synthetic peptide (Fig. 1) was monitored by ^{13}C NMR in the presence of 0, 0.5, 1, 1.5, 2, 4, 8, 20, and 40 mM MMPC. The pH was kept at 4 in these experiments. Similar control titrations were conducted in which the fluorescence emission and steady-state anisotropy of W19 in MLT were determined versus lipid concentration (20 μM MLT, 10 mM 4-morpholinepropanesulfonic acid, 10 mm KCl at pH 7), with lipid:peptide molar ratios varying from 1:1 to 250:1. Note that in the fluorescence experiments, the MLT concentration was ~50 times less than that needed for NMR. Given the unavoidable and certain sensitivity of the system to the concentrations of both the peptide and the lipid, extrapolations from the fluorescence results to those from NMR could be problematic. We show here, however, that there did not seem to be a problem in these particular experiments.

In additional ^{13}C- and ^{31}P-NMR measurements, the pH of MMPC micelle solutions and of solutions of micelle-bound MLT was adjusted from 4 to 11 by successive additions of aliquots of 1 N NaOH solution. Care was taken with the pH adjustments because of the sensitivity of MMPC acyl esters to base-catalyzed hydrolysis and the possibility of acyl chain or phosphocholine headgroup migration of MMPC (Fischgold and Chain, 1934; Plückthun and Dennis, 1982). ^{31}P-NMR data indicated that there was less than 10% decomposition of MMPC during our experiments; furthermore, the overall structure of the MMPC micelles was apparently not affected by pH, as evidenced by the constancy of their ^{13}C chemical shifts. Finally, the pH of each sample was tested immediately before and after a given NMR measurement; in all cases the final pH values deviated by less than ±0.2 unit from their original values. Note that the pH values given are direct meter readings without correction for isotope effects.

NMR relaxation data analysis

The ^{13}C relaxation parameters T_1 and NOE depend upon the magnetic dipolar interaction of the ^{13}C nucleus with its attached proton(s) and upon

the CSA of the ^{13}C; they are given by (Abragam, 1961)

$$T_1^{-1} = R_{DD} + R_{CSA}, \quad (1)$$

and

$$NOE = 1 + \frac{1}{4} n\alpha^2 \frac{\gamma_H}{\gamma_C}\left[\frac{6J(\omega_H + \omega_C) - J(\omega_H - \omega_C)}{R_{DD} + R_{CSA}}\right], \quad (2)$$

where

$$R_{DD} = \frac{1}{4} n\alpha^2[J(\omega_H - \omega_C) + 3J(\omega_C) + 6J(\omega_H + \omega_C)] \quad (3)$$

$$R_{CSA} = \frac{1}{3} \beta^2 J(\omega_C), \quad (4)$$

with

$$\alpha = \frac{\gamma_C \gamma_H \hbar}{r_{CH}^3} \quad \text{and} \quad \beta = \frac{3}{2} \omega_C \delta_{ZZ}\left(1 + \frac{\eta^2}{3}\right)^{1/2}.$$

ω_C and ω_H are the carbon and proton resonance frequencies, γ_C and γ_H are their respective gyromagnetic ratios; $\hbar$ is Planck's constant over 2π, r_{CH} is the carbon-proton distance, δ_{ZZ} is the largest magnitude principal element of the ^{13}C-CSA tensor (in ppm), n is the number of bonded protons, and η is the CSA tensor asymmetry parameter.

The spectral density, $J(\omega)$, following Lipari and Szabo (1982), is

$$J(\omega) = \frac{2}{5}\left[\frac{S^2\tau_m}{1 + \omega^2\tau_m^2} + \frac{(1 - S^2)\tau}{1 + \omega^2\tau^2}\right], \quad (5)$$

where S^2 is a generalized, motional model-free order parameter dependent on the amplitude of the internal motion of the C-H vector ($0 \le S^2 \le 1$), and $\tau^{-1} = \tau_m^{-1} + \tau_e^{-1}$ consists of τ_e, an effective correlation time for the internal motion, which has meaning when $S^2 < 1$, and τ_m, a correlation time for the overall rotational motion of the molecule. When $S^2 = 1$, the C-H vector shows no internal motion, and generally as $S^2 \to 0$, the motion becomes freer. Only a single parameter (τ_m) is used to characterize the overall tumbling, because that motion is expected to be isotropic for MMPC micelles, which are presumed to be nearly spherical. Values of τ_m, S^2, and τ_e were found from $1/T_1$ and NOE measured at two frequencies by least-squares fitting of the measured relaxation values to Eqs. 1–4, using Eq. 5 for the spectral density. CSA parameters used in the analysis are listed in Table 1.

TABLE 1 CSA parameters used for amino acids in the analysis of dynamics

Nucleus	δ_{ZZ} (ppm)	η
G-Cα*	20.2	0.916
A-Cα‡	−19.3	0.415
L-Cα§	−19.3	0.415
K-Cϵ§	−20.7	0.580
W-Cδ_1¶	78.3	0.932
W-Cϵ_3‖	−115	0.639

*Haberkorn et al. (1981).
‡Naito et al. (1981). Leucine was treated as the same as alanine.
§Calculated by using "typical" values for methylene compiled by Duncan (1990).
¶Separovic et al. (1991).
‖F. Separovic, unpublished results.

RESULTS AND DISCUSSION

^{13}C-NMR and fluorescence spectral observations of the MMPC-MLT complex

Lipid titration of MLT

Shown in Fig. 2 is the titration of the ^{13}C chemical shifts of 1 mM MLT (peptide (iii) in Fig. 1 with ^{13}C enrichment at G3-α, L9-α, A15-α, and K21-ϵ) with MMPC varied from 0 to 40 mM in 50 mM phosphate at pH 4. Resonance assignments were based upon comparison of the spectra among the various peptides, some of which contained only a single $^{13}C\alpha$-labeled residue; upon the fact that specific amino acid residues have similar $^{13}C\alpha$ chemical shifts in common environments; upon known differences in Cα, Cϵ, and aromatic ^{13}C chemical shifts (e.g., see Wishart et al., 1995); and upon previous work in our laboratories (Buckley et al., 1993; Kemple et al., 1994). From Fig. 1 it can be seen that the resonance position of K21-Cϵ remained nearly unchanged in the course of the lipid titration, whereas substantial chemical shift changes and, at low lipid:MLT ratios, two separate peaks were observed for the resonances of G3-Cα, L13-Cα, and A15-Cα. Considerable line broadening occurred for all four nuclei, which, together with the chemical shift changes, indicates the formation of lipid-MLT complexes. No further chemical shift changes were seen beyond lipid:peptide ratios of 4:1, and then only a single resonance was observed for each of the four labeled sites, suggesting that the micelle-bound MLT adopts predominantly one conformational state. The existence of two peaks for G3-Cα, L13-Cα, and A15-Cα at lipid:MLT molar ratios below 4:1 indicates that free, random-coil MLT and lipid-interacting MLT were in slow exchange on the NMR chemical shift time scale. The exchange rates in those instances were estimated to be ~200–425 s^{-1} from simulations of the lineshapes. Studies of MLT with ^{13}C enrichment at other sites gave similar results; all of the measured chemical shifts are given in Table 2. These α-carbon chemical shifts are consistent with a mainly α-helical conformation of MLT in the presence of lipid (see below). The Cϵ chemical shifts of K7, K21, and K23; the Cα-G1 chemical shift; and the Cδ_1- and ϵ_3-W19 chemical shifts were less affected by lipid interaction. Resonances from ^{13}C at natural abundance in the lipid itself were well resolved from those of MLT.

Titration of the MLT trp steady-state anisotropy with lipid is shown in Fig. 3. The "break" point in the plot at a lipid:peptide molar ratio of about 30 and the stable signal at higher ratios strongly support the notion of a stable mixed micelle at ratios above 30. These results are consistent with results we have reported earlier in less extensive measurements (Weaver et al., 1992). The lower anisotropy values at molar ratios below 30 probably derive from the existence of at least two species of melittin, free and complexed, exchanging slowly on the fluorescence time scale. In such a situation the measured steady-state anisotropy $r_{ss,m} = f_1 r_1 + f_2 r_2$, where r_1 and r_2 refer to the anisotropy expected for

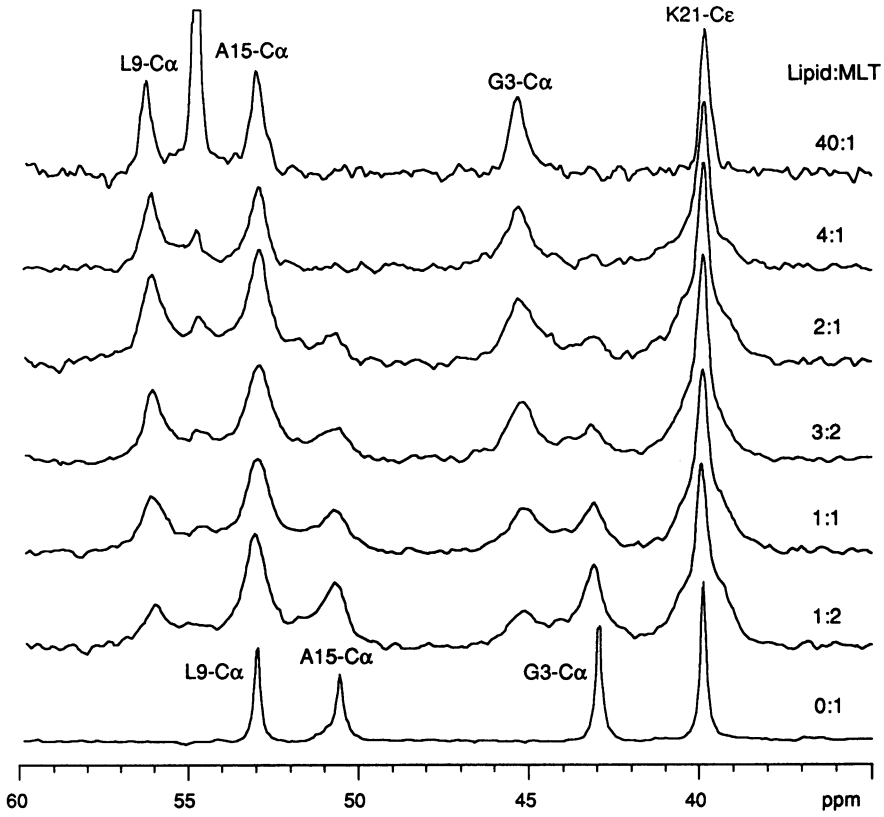

FIGURE 2 Proton-decoupled ^{13}C-NMR spectra for MMPC lipid titration of 1 mM MLT (peptide (iii) in Fig. 1) in 50 mM phosphate buffer at pH 4 obtained at 125.7 MHz. Chemical shifts are referenced to external dioxane at 67.37 ppm. The molar ratios of MMPC lipid to MLT are 40:1, 4:1, 2:1, 3:2, 1:1, 1:2, and 0:1 from top to bottom. The signals in the spectrum at the bottom are L9-Cα, A15-Cα, G3-Cα, and K21-Cε from left to right. The peptide signals in the spectrum at the top, which corresponds to an MMPC/MLT ratio of 40:1, are L9-Cα (56.24 ppm), A15-Cα (53.00 ppm), G3-Cα (45.36 ppm), and K21-Cε (39.83 ppm). The other signal is from natural abundance ^{13}C in the MMPC lipid. The temperature of the sample was 25°C.

the trp residue exclusively in each of the environments, and f_1 and f_2 are the intensity weighted fractions of the two. Because the anisotropy of uncomplexed, monomeric MLT is very low, the overall anisotropy must increase progressively with the formation of the complex, as seen in Fig. 3. Confirming results were found from the dependence of the fluorescence spectra on the lipid:peptide ratio as well (not shown).

There are substantial differences in sample conditions in the NMR and fluorescence titrations. In fluorescence, the lipid concentration is below the CMC (~70 μM, Stafford et al., 1989) at the low lipid:peptide ratios, and it is likely that

TABLE 2 ^{13}C chemical shifts in ppm of melittin in different environments

Nucleus	Coil pH 4	Helical CD_3OD	MMPC-MLT complex pH 4	pH 7	pH 9	pH 11
G1-Cα	41.06	41.84	41.30	41.70	43.86	
G3-Cα	42.93	45.69	45.36	45.31	45.25	45.24
A4-Cα	50.34	53.97	52.87	52.82	52.82	
L6-Cα	52.97	57.23*	56.14			
L9-Cα	52.99	56.55	56.24	56.18	56.28	56.25
G12-Cα	43.00	44.49	44.53	44.52	44.59	
L13-Cα	51.46	58.46*	57.62	57.62	57.62	57.71
A15-Cα	50.55	53.90	53.00	52.96	52.98	53.10
L16-Cα	53.48	57.60*	56.21	56.21	56.25	56.25
W19-$C\delta_1$	124.98		125.18	125.18	125.18	125.08
W19-$C\epsilon_3$	118.84	118.64	118.61	118.61	118.62	
K7-Cε	39.88		39.96	39.99	40.02	40.36
K21-Cε	39.90	39.95	39.83	39.75	39.82	40.54
K23-Cε	39.80		39.79	39.74	39.78	40.64

No entry means that no measurement was performed. Chemical shifts were referenced to external dioxane at 67.37 ppm and were reproducible to ±0.05 ppm.

*From Buckley et al. (1993).

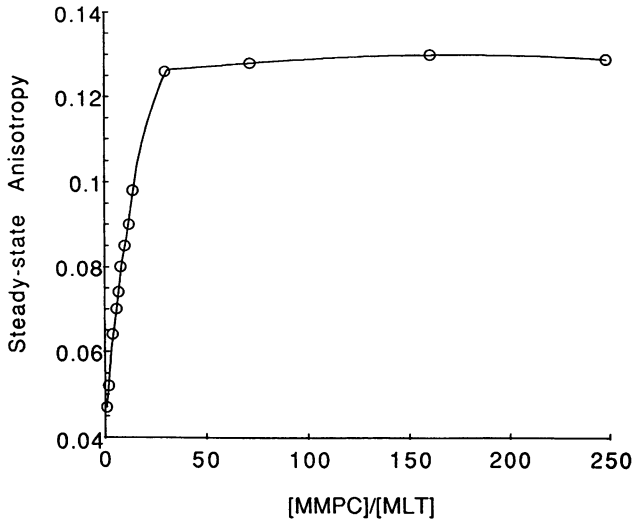

FIGURE 3 Tryptophan steady-state anisotropy of MLT-MMPC complexes at 20°C at excitation and emission wavelengths of 300 nm and 340 nm, respectively. The curve shown is only to aid visualization and does not represent a fit of any theoretical expression to the data. Sample conditions were 20 μM MLT, 10 mM 4-morpholinepropanesulfonic acid, 10 mM KCl at pH 7 with MMPC varied to obtain the lipid:peptide ratios shown.

a mixed micelle is formed that is dominated by peptide but is responsible for only a fraction of the melittin, with much of the melittin remaining free. As the lipid concentration increases, the composition of the micelle changes until a final form appears at lipid-to-peptide ratios in excess of 30:1. Because the NMR experiments are conducted at concentrations of MMPC that at the outset are greater than the CMC, the path to a final form at high lipid-to-peptide ratios might be different in the fluorescence and NMR experiments (Fig. 2). Given these considerations and the observation from NMR that the chemical shifts of MLT remain unchanged at lipid-to-peptide ratios above 4:1, the complex formed at the lipid-to-peptide ratio of 40:1 was chosen for the majority of the NMR measurements.

QLS at 20°C of 1.5 mM MMPC micelles in 50 mM phosphate at pH 7 revealed the diameter of the micelles to be ~4.5 nm devoid of peptide and ~5.5 nm in the presence of melittin at a lipid-to-peptide ratio of about 40:1. The standard deviation in these measurements was 0.5 nm, and the full widths at half-maximum of the analyzed scattering curves were ~1.4 nm. There was no evidence of significant heterodispersity in size in the MLT-bound micelles. It seems likely that the increment in size when peptide is present derives simply from the addition of the peptide per se to the micelle rather than from an increase in the number of lipid molecules in each micelle, i.e., the "aggregation" number of the lipid in the micelle. Similar sizes for MLT-DPC micelle complexes sizes were reported by Lauterwein et al. (1979).

Influence of pH on ^{13}C-NMR spectra

Natural abundance ^{13}C-NMR spectra of the MMPC micelles indicated that the micelles were very stable over a broad pH range. No changes in either chemical shift or linewidth of any of the MMPC resonances were observed between pH 4 and pH 11 in the absence of MLT. In the presence of MLT, the ^{13}C chemical shifts of the MMPC were insensitive to changes in pH, apart from the appearance of a few additional lower intensity signals at pH 11, and the linewidths were unchanged. Our results are consistent with the observation by Hauser et al. (1975) that the packing density of phosphatidylcholine monolayers and bilayers is independent of pH over a wide range. The measured chemical shifts of ^{13}C-labeled MLT (Table 2) were the same at pH 4, 7, and 9 (except for the Cα of G1; see below), and only line-broadening consistent with formation of the lipid-peptide complex was observed. At pH 11 (see later) the MLT signals showed a substantial increase in linewidth.

The conformation of MLT bound to MMPC micelles

Wishart et al. (1991) have published a summary of the correspondence between ^{1}H, ^{13}C, and ^{15}N NMR chemical shifts and secondary structure in over 70 proteins. They recognized that ^{13}C chemical shifts correlate well with secondary structure, particularly with helical regions, an inference corroborated for ^{13}C and ^{1}H in MLT by Buckley et al. (1993). Spera and Bax (1991) also reported a strong correlation between Cα and Cβ chemical shifts and the backbone conformation in proteins of well-defined structure, and Reily et al. (1992) have demonstrated agreement between changes in ^{13}Cα chemical shifts and the magnitude of the molar ellipticity at 220 nm of the circular dichroism spectrum of the 14 amino-acid peptide bombesin in 2,2,2-trifluoroethanol. Thus, the validity of the ^{13}Cα chemical shift as an indicator of peptide or protein secondary structure seems established, and its use as such has the advantage of giving site-specific information.

Of the eight α-carbons of MLT (excluding G1) examined by ^{13}C NMR in the MMPC-MLT micelles, three have chemical shifts within 0.3 ppm of their values in methanol (Table 2), where MLT is known to be nearly completely α-helical (Buckley et al., 1993), whereas the chemical shifts of the other five differ from their methanol values by at most 1.4 ppm. All of the α-carbon resonances examined shifted downfield substantially (including G1 at pH 9) relative to their positions in random-coil MLT, with the largest shift of over 6 ppm occurring for the L13-Cα. The chemical shift values are consistent with those listed by Wishart et al. (1991) for α-helical structures and thus strongly suggest then that residues 1 to 16 of MLT are α-helical (apart from a presumed kink at residues 11 and 12; Inagaki et al., 1989; Ikura et al., 1991) in the MMPC micelle environment. Furthermore, the stability of the measured α-carbon chemical shifts from pH 4 to pH 11 (Table 2) indicates that the α-helical conformation of residues 1–16 in the micelle-bound MLT is preserved over this pH range. The predominance of the helix is consistent with the 2D NMR results of Ikura et al. (1991) for MLT in DPC mixed micelles, which

showed MLT to be nearly completely helical in those micelles. No direct information on the conformation of residues beyond L16 was available from our experiments, because we did not have any α-carbon-labeled residue to examine, and the $^{13}C\epsilon$ chemical shifts of the lys residues changed little on MLT binding to the micelles at pH 4, 7, and 9 (see below) and in any event are independent of peptide secondary structure. (In measurements on MLT in aqueous solutions, the chemical shifts of the $^{13}C\epsilon$ resonances of K7, K21, and K23 were not affected by tetramer formation (P. Buckley, private communication) and hence were not dependent on MLT secondary structure.)

G1 shows a large change in chemical shift between pH 7 and pH 9, which reflects the pK_a of the MLT N-terminus. In particular, Zhu et al. (1995b) have measured the pK_a of the α-amino group of G1 of MLT for MLT bound to MMPC micelles and free in solution and found the pK_a to be 7.9 in both cases, which is comparable to other reported values for this residue in simple solutions of MLT (7.3 by Wilcox and Eisenberg, 1992; 7.35 by Goto and Hagihara, 1992; 7.8 by Lauterwein et al., 1980). The binding of MLT to the lipid surface apparently does not influence protonation of the N-terminus amino group, and MLT can bind when the amino-terminus is either cationic (and thus is unable to penetrate into the micellar interior) or neutral.

The MMPC titration of MLT (Fig. 2) shows that at a lipid-to-MLT ratio of 4:1, residues 1–16 have reached their final, nearly completely α-helical conformation, judging by the disappearance of peaks corresponding to free, random-coil MLT. However, signals representative of α-helical MLT are clearly present, even at lipid-to-MLT ratios as low as 1:2. We infer that mixed micelles of as yet undefined composition and form exist at the lower lipid-to-peptide ratios, at least at the concentrations of peptide and lysolipid used for the NMR experiments. Given the structural response of MLT to the lipid at these low ratios, we propose that hydrophobic interactions are of primary importance in driving the peptide's conformational changes, an inference consistent with that of de Kroon et al. (1991) in their studies of the interaction of other amphiphilic peptides with model membranes.

A question arises as to whether the α-helical MLT formed in the pH 4 titration could be a tetramer triggered by the MLT-lipid interaction. The available evidence does not favor MLT forming a tetramer under these conditions: i) MLT at 1 mM concentration is a monomer in water or even in 50 mM phosphate at pH 4 (unpublished result); ii) it is unlikely that the lipid headgroup could sufficiently counteract the positive charges on MLT to trigger tetramer formation, especially at low lipid-to-MLT ratios and low MLT concentration; iii) MLT is a monomer when fully bound to DPC micelles (Inagaki et al., 1989) and to the internal surface of reversed sodium bis(2-ethyl-1-exyl)sulfosuccinate micelles (Bismuto et al., 1993).

^{13}C chemical shifts of the MLT side chains (Table 2) are potentially sensitive to relative solvent exposure in the micellar bound state. An upfield change of ~0.2 ppm was observed for the W19-ϵ_3 carbon of MLT in methanol and in the MMPC mixed micelle. These shifts are compatible with partial partitioning of this part of the trp side chain into the relatively less polar micellar acyl chain environment, which could resemble bulk methanol in terms of dielectric permittivity (Gierasch et al., 1982). On the other hand, an opposite, downfield shift of 0.2 ppm was found for W19-$C\delta_1$ of MLT in the micelle. This indicates that the immediate environment of the $C\delta_1$ differs from that of $C\epsilon_3$, but the chemical shift would also reflect hydrogen bonding of the indole nitrogen with the MMPC headgroups (Chattopadhyay and Rukmini, 1993). Small to negligible changes in chemical shift were observed for the lys-$C\epsilon$ resonances in the micellar bound state at pH 4 relative to free MLT, indicating that the polarity of the environment of the lys side chains is not appreciably altered by lipid binding, i.e., that the lys side chains remain exposed to solvent. Electron spin resonance studies on MLT spin-labeled at the amino terminus and at the lys ϵ-amino moieties have shown the side chain of K7 to be the most exposed to solvent, followed by those of K23 and K21 (Altenbach and Hubbell, 1988) in order. Admittedly, spin labeling rendered these moieties non-ionic, but even so there was no apparent influence on the extent of interaction of the lysine side chains with water.

The orientation of MLT bound to MMPC micelles

Conflicting results have been reported about the orientation of the MLT helix relative to the membrane plane (Vogel, 1987; Brauner et al., 1987; Stanislawski and Rüterjans, 1987; Altenbach and Hubbell, 1988). Recent work by Frey and Tamm (1991) suggested that the orientation of MLT in membranes depends on the degree of hydration of the model membranes rather than on the technique used for its determination. They found that the MLT α-helix was preferentially oriented parallel to the plane of the bilayer in a single membrane sample but parallel to the phospholipid acyl chains when the membranes were stacked in multi-bilayers. Results consistent with that interpretation have been provided by Smith et al. (1994) on ^{13}C-enriched peptide carbonyl groups of MLT incorporated into bilayers of the diether lipid ditetradecylphosphatidylcholine aligned between stacked glass plates.

Although our data do not provide direct evidence for orientation, there is indirect evidence that the peptide may be largely on the surface. This inference derives from the apparent invariance of the interaction of the lysyl amino groups of MLT with solvent in lipid-free and micellar-bound lipid MLT. The Nζ remains cationic at pH $\leq$ 9 (Zhu et al., 1995b) and hence is unlikely to penetrate substantially into the micelle interior. Obviously, with micelles we have to be somewhat cautious with this supposition because of the depth to which water might penetrate between the lysolipid moieties, which could bias our inference. However, the most practical conclusion is that the mixed micelle is stabilized by van der Waal's interactions between the amino acid side chains (especially those of leu and ile residues) and the fatty acyl moieties, and a simple model then sug-

gests primarily an orientation along the surface. On the other hand, the orientation of the first half of the molecule, residues 1–12, from the N-terminus to the "hinge," might be influenced substantially by the ionic state of the α-NH_2 of G1. Upon deprotonation G1 might indeed penetrate more substantially into the micelle interior, taking with it the MLT tail.

^{31}P-NMR observations of phosphate and MMPC interactions with MLT

Chemical shifts and linewidths

Phosphate interacts strongly with MLT (Drake and Hider, 1979; Strom et al., 1980; Podo et al., 1982; Wilcox and Eisenberg, 1992). The binding of cationic MLT to a zwitterionic MMPC micelle will almost inevitably lead to a conformational change of the choline headgroup of the lipid. Accordingly, it is possible that ^{31}P chemical shifts and linewidths of the phosphoryl group of the MMPC micelle and of solvent (or bound) phosphate groups would be useful probes of charge-charge interactions in the MLT-lysolipid mixed micelle. ^{31}P-NMR spectra were gathered over the pH range of 4 to 11, and only two signals, one assigned to MMPC and the other to free phosphate using their T_1 values, were observed. For both the MMPC and the MMPC-MLT micelles, the chemical shift of free phosphate was strongly pH dependent, whereas the chemical shift of the MMPC phosphoryl group was not. Because only a single line whose position was independent of MLT concentration was observed from the phosphate and the MMPC headgroup, no information on the interaction of MLT with either was provided from their chemical shifts. However, their linewidths were dependent on the presence of MLT, as indicated in Table 3, where $\Delta\nu_{\text{phos-mlt}}$ and $\Delta\nu_{\text{mmpc-mlt}}$, representing the differences in the linewidths in the presence and absence of MLT, are given. Note that there was little change in these linewidths with pH without MLT, and therefore the larger linewidths of the phosphate and MMPC in the presence of MLT are reasonable indicators of the interaction of both phosphate and the micelle headgroup with MLT. The change in $\Delta\nu_{\text{phos-mlt}}$ and $\Delta\nu_{\text{mmpc-mlt}}$ with pH suggests that these interactions are electrostatic in nature.

MLT-phosphate ion interaction

Podo et al. (1982) found that phosphate "binds" with MLT in aqueous solution with a stoichiometry of 5–6 phosphate ions (monovalent at pH 7.0) per MLT molecule. In a MLT-MMPC mixed micelle the number of "binding sites" for phosphate on MLT will likely be reduced by the interaction of the cationic charges in MLT with the phosphoryl group of the MMPC lipid. A complicated pH dependence for MLT-phosphate interaction is then expected because i) phosphate ions change from monovalent to divalent at pH 7.21 (Weast, 1983); and ii) the number of positive charges (roughly equivalent to the number of phosphate "binding sites") on MLT will be reduced from six to two as the pH approaches 11. Even so, a clear picture of the MLT-phosphate interaction can be deduced from an analysis of the linewidth data in Table 3. Our argument is as follows.

The interaction of phosphate with MLT involves both anion "binding" and electrostatic screening. In principle, at low pH, phosphate ions can interact with all six positively charged sites on MLT despite the competition from the phosphoryl group of MMPC. In particular, phosphate ions have relatively high affinity for the guanidinium groups of the arginine residues because of their ability to form a quasi-ring structure linked through hydrogen bonding and electrostatic interactions (Rifkind and Eichhorn, 1970; Ichimura et al., 1978). The charge on the guanidinium group is known to be stabilized by interactions with anions of tetrahedral geometry such as ClO_4^-, $H_2PO_4^-$, $HPO_4^=$, and $SO_4^=$ (Ichimura et al., 1978). As shown in Fig. 4, $\Delta\nu_{\text{phos-mlt}}$ is virtually unchanged from pH 4 to pH 7, implying that the cation sites of MLT are fully exposed to phosphate. The considerably reduced $\Delta\nu_{\text{phos-mlt}}$ at pH 8 most likely reflects deprotonation of the N-terminus of MLT, which has a pK_a of 7.9 in MMPC micelles (Zhu et al., 1995b), and suggests strongly that the N-terminus of MLT is one of the sites that phosphate ions predominantly bind. The value of $\Delta\nu_{\text{phos-mlt}}$ is gradually reduced to 0.7 Hz at pH 11, apparently because of the deprotonation of the three lysine side chains (Zhu et al., 1995b). Thus, interaction of phosphate ions with at least one of the lys side chains is indicated, but no information on specificity is present.

TABLE 3 ^{31}P-NMR lineshape analysis of phosphate and of the phosphoryl groups of MMPC with and without MLT

	Linewidth of phosphate (Hz)			Linewidth of MMPC micelle (Hz)		
pH	With MLT	Without MLT	$\Delta\nu_{\text{phos-mlt}}$	With MLT	Without MLT	$\Delta\nu_{\text{mmpc-mlt}}$
4	18.8	7.3	11.5	12.4	10.5	1.9
5	17.9	7.5	10.4	11.8	10.2	1.6
6	23.1	9.3	13.8	11.7	9.7	2.0
7	22.7	10.0	12.7	11.5	9.6	1.9
8	14.5	8.9	5.6	11.6	9.2	2.4
9	12.2	8.4	3.8	11.3	9.2	2.1
10	9.8	8.1	1.7	10.9	9.4	1.5
11	8.6	7.9	0.7	9.5	9.4	≈0

Linewidths are the full width at half-maximum intensity of the resonances. The standard error in their values is 0.2 Hz.

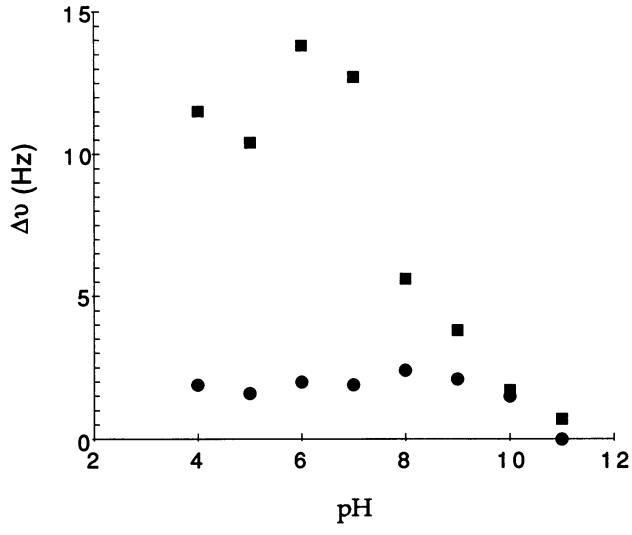

FIGURE 4 pH dependence of $\Delta\nu_{phos\text{-}mlt}$ (■) and $\Delta\nu_{mmpc\text{-}mlt}$ (●).

MLT-MMPC headgroup interaction

The binding of MLT to MMPC micelles will likely induce a conformational change of the lipid headgroup due to MLT's positive charge, evidence for which is provided from deuterium NMR studies (Kuchinka and Seelig, 1989; Roux et al., 1989; Dempsey et al., 1989; Beschiaschvili and Seelig, 1990).

The electrostatic contribution to the MLT-membrane interaction has been investigated quantitatively (Schwarz and Beschiaschvili, 1989; Kuchinka and Seelig, 1989; Beschiaschvili and Seelig, 1990; Stankowski and Schwarz, 1990). The effective charge of MLT as sensed by the membrane system near neutral pH was determined to be around +2, instead of +5 or +6. The result was explained by postulating that only two of the charged groups of MLT interact with the membrane, whereas the others remain in the aqueous phase, fully screened by counter-ions. Our linewidth data are consistent with this hypothesis. The $\Delta\nu_{mmpc\text{-}mlt}$ values remain invariant until pH 11, as can be seen in Fig. 4, implying that a constant charge on MLT was sensed by the MMPC micelle, whereas the $\Delta\nu_{phos\text{-}mlt}$ shows a sharp drop above 7, as noted earlier.

Relaxation measurements and motional parameters of micelle-bound MLT

Overall correlation time

Having established MMPC micelle stability over a broad pH range, and having satisfied ourselves that the MMPC-MLT micelle is also stable and likely has MLT in a helical conformation, we made ^{13}C relaxation measurements to determine peptide main-chain and side-chain dynamics. ^{13}C-T_1 and NOE values were measured for micelle-bound MLT at 25°C at both 75.4 and 125.7 MHz at pH 4, 7, 9, and 11. The data are shown in Table 4 and the results of their analysis are summarized in Table 5. At pH 11, relaxation measurements were made only on the three lys side chains, to minimize the length of exposure of the samples to those very basic conditions.

The overall correlation time, τ_m, fit as a common parameter within each data set including all of the available data, was found to be 10 ns with a standard error of 2 ns at pH 4, 7, and 9, and 16 ± 3 ns at pH 11. The values found for τ_m at pH 4, 7, and 9 agree well with those near 11 ns inferred by Weaver et al. (1992). Furthermore, from the Stokes-Einstein-Debye relation and the QLS measurement of the diameter of the micelles (5.5 nm with MLT and 4.5 nm without), we calculate respective expected τ_m values of 21.2 ns and 11.6 ns at 25°C based on the viscosity of water. The calculated value of τ_m for the mixed micelle is larger than the experimental value of 10 ns. Because micelles are loosely packed, flexible particles, this outcome is not unexpected. The differences may also reflect the inherent difficulty in calculating τ_m as well as in measuring micelle size accurately.

Backbone dynamics of micelle-bound MLT

In general, similar order parameters were observed across the length of the MLT helix (residues 1 through 16) in the micelle-peptide complexes at pH 4, 7, and 9, as illustrated in Table 5 and Fig. 6. The averages of the order parameters of the Cα-H vectors are, respectively, 0.66, 0.70, and 0.69 at pH 4, 7, and 9, which suggests that the bound MLT, although somewhat constrained in the micelle, retains considerable backbone mobility; the order parameters reported here are small compared with those normally found in proteins, except in particularly flexible regions (see for example, Barbato et al., 1992; Mandel et al., 1995). On the other hand, these S^2 values are considerably larger than those found for monomeric random-coil or even tetrameric MLT (~0.4) and are comparable to values found for monomeric helical MLT in methanol (P. Buckley, manuscript in preparation). There is no clear pH dependence of the Cα-H order parameters. The differences in S^2 and τ_e values between pH 4, 7, and 9 for a given residue are mostly explained by the uncertainties in the measured T_1 and NOE values (Table 4). The uncertainties (standard errors) listed in Table 5 for S^2 and τ_e were determined by fixing τ_m once its value was found from fits in which all of the parameters had been allowed to vary; thus they reflect variations within a set of data at a given pH. The standard errors in S^2 and τ_e were on the order of 20% and 5–50%, respectively, in the fits in which τ_m also varied.

At a given pH, order parameters for residues G12, L13, A15, and L16 were smaller than those of G3, A4, L6, and L9. This is shown in Fig. 5, where the average values of S^2 at pH 4, 7, and 9 for each residue (except L6, for which there are data only at pH 4) are shown along with their standard deviations. Apparently micelle-bound MLT is more flexible from G12 onward, at least through L16. This correlation was not seen for MLT as a monomeric random coil, as a monomeric helix in methanol, or as a tetramer (P.

TABLE 4 Relaxation measurement of the MMPC micelle-bound MLT at different pH values

Nucleus	125.7 MHz T_1 (s)	125.7 MHz NOE	75.4 MHz T_1 (s)	75.4 MHz NOE
		pH 4		
G1-Cα	0.38 (1)	1.55 (3)	0.21 (1)	1.6 (1)
G3-Cα	0.44 (2)	1.34 (2)	0.22 (1)	1.47 (3)
A4-Cα	0.78 (6)	1.40 (6)	0.39 (1)	1.58 (7)
L6-Cα	0.87 (1)	1.42 (2)	0.46 (1)	1.40 (8)
L9-Cα	0.86 (1)	1.33 (6)	0.47 (1)	1.31 (4)
G12-Cα	0.50 (1)	1.34 (2)	0.33 (1)	1.28 (4)
L13-Cα	1.02 (3)	1.35 (3)	0.57 (2)	1.5 (1)
A15-Cα	1.05 (8)	1.38 (5)	0.52 (2)	1.44 (3)
L16-Cα	1.08 (2)	1.36 (3)	0.52 (1)	1.53 (4)
W19-$C\epsilon_3$	0.78 (2)	1.20 (5)	0.43 (1)	1.54 (1)
W19-$C\delta_1$	0.59 (4)	1.40 (5)	0.38 (3)	1.6 (1)
K7-Cε	0.42 (1)	2.39 (1)	0.32 (1)	2.42 (2)
K21-Cε	0.32 (1)	2.12 (9)	0.25 (1)	2.3 (2)
K23-Cε	0.33 (2)	2.04 (8)	0.20 (1)	2.08 (5)
		pH 7		
G1-Cα	0.38 (2)	1.5 (1)	0.19 (1)	1.44 (7)
G3-Cα	0.43 (1)	1.36 (5)	0.22 (1)	1.34 (3)
A4-Cα	0.81 (1)	1.37 (2)	0.42 (1)	1.40 (2)
L9-Cα	0.88 (7)	1.38 (3)	0.44 (2)	1.38 (3)
G12-Cα	0.47 (2)	1.3 (1)	0.26 (2)	1.40 (4)
L13-Cα	1.07 (8)	1.36 (7)	0.59 (2)	1.53 (1)
A15-Cα	1.04 (6)	1.44 (5)	0.55 (4)	1.38 (3)
L16-Cα	1.06 (5)	1.37 (3)	0.46 (2)	1.43 (5)
W19-$C\epsilon_3$	0.68 (2)	1.18 (5)	0.45 (3)	1.32 (3)
W19-$C\delta_1$	0.52 (4)	1.37 (5)	0.38 (1)	1.41 (4)
K7-Cε	0.42 (1)	2.37 (0)	0.33 (1)	2.27 (1)
K21-Cε	0.33 (1)	2.19 (3)	0.25 (1)	2.3 (2)
K23-Cε	0.31 (2)	2.05 (6)	0.20 (1)	2.07 (5)
		pH 9		
G1-Cα	0.37 (3)	1.51 (1)	0.26 (2)	1.5 (1)
G3-Cα	0.41 (2)	1.31 (5)	0.21 (1)	1.33 (5)
A4-Cα	0.79 (2)	1.39 (5)	0.46 (1)	1.48 (8)
L9-Cα	0.88 (1)	1.36 (5)	0.36 (2)	1.44 (8)
G12-Cα	0.44 (1)	1.44 (3)	0.27 (1)	1.40 (8)
L13-Cα	1.11 (5)	1.31 (5)	0.53 (4)	1.43 (8)
A15-Cα	1.03 (5)	1.43 (3)	0.53 (3)	1.49 (8)
L16-Cα	0.94 (5)	1.35 (1)	0.50 (2)	1.54 (7)
W19-$C\epsilon_3$	0.58 (2)	1.21 (4)	0.45 (3)	1.32 (3)
W19-$C\delta_1$	0.57 (4)	1.39 (4)	0.37 (3)	1.37 (4)
K7-Cε	0.43 (1)	2.38 (1)	0.33 (0)	2.3 (1)
K21-Cε	0.32 (0)	2.14 (7)	0.23 (0)	2.29 (5)
K23-Cε	0.31 (1)	1.98 (4)	0.21 (0)	2.03 (7)
		pH 11		
K7-Cε	0.35 (2)	2.11 (3)	0.28 (1)	2.1 (1)
K21-Cε	0.30 (2)	2.09 (5)	0.22 (1)	2.1 (1)
K23-Cε	0.29 (0)	2.06 (6)	0.19 (1)	2.0 (1)

Data shown here represent the average of at least two measurements, and the numbers in parentheses denote the magnitude of the deviation in the last digit shown. The temperature was 25 ± 0.5°C. The chemical shifts are listed in Table 2.

TABLE 5 The motional parameters for the backbone and side chain of MMPC micelle-bound MLT at different pH values

Nucleus	pH 4 τ_m = 10 ± 2 ns χ^2 = 0.013 S^2	pH 4 τ_e (ps)	pH 7 τ_m = 10 ± 2 ns χ^2 = 0.011 S^2	pH 7 τ_e (ps)
G1-Cα	0.69 (2)	73 ± 6	0.82 (4)	94 ± 21
G3-Cα	0.74 (2)	41 ± 5	0.77 (3)	38 ± 4
A4-Cα	0.78 (2)	82 ± 11	0.79 (1)	53 ± 3
L6-Cα	0.71 (1)	39 ± 1		
L9-Cα	0.74 (2)	30 ± 2	0.75 (3)	39 ± 7
G12-Cα	0.54 (2)	15 ± 1	0.66 (3)	24 ± 4
L13-Cα	0.57 (2)	24 ± 2	0.54 (2)	23 ± 2
A15-Cα	0.62 (2)	23 ± 3	0.59 (3)	23 ± 3
L16-Cα	0.60 (1)	25 ± 1	0.68 (3)	25 ± 4
W19-$C\epsilon_3$	0.63 (1)	30 ± 2	0.69 (2)	23 ± 3
W19-$C\delta_1$	0.73 (4)	99 ± 20	0.81 (2)	120 ± 19
K7-Cε	0.19 (1)	59 ± 2	0.21 (1)	56 ± 1
K21-Cε	0.28 (3)	83 ± 3	0.28 (2)	81 ± 3
K23-Cε	0.47 (3)	99 ± 8	0.47 (3)	106 ± 9

Nucleus	pH 9 τ_m = 10 ± 2 ns χ^2 = 0.015 S^2	pH 9 τ_e (ps)	pH 11 τ_m = 16 ± 3 ns χ^2 = 0.013 S^2	pH 11 τ_e (ps)
G1-Cα	0.61 (3)	49 ± 7		
G3-Cα	0.82 (3)	46 ± 6		
A4-Cα	0.71 (2)	50 ± 3		
L9-Cα	0.86 (3)	73 ± 7		
G12-Cα	0.62 (2)	32 ± 3		
L13-Cα	0.62 (3)	19 ± 3		
A15-Cα	0.60 (2)	28 ± 3		
L16-Cα	0.64 (2)	34 ± 3		
W19-$C\epsilon_3$	0.70 (2)	33 ± 3		
W19-$C\delta_1$	0.84 (3)	118 ± 35		
K7-Cε	0.21 (1)	56 ± 2	0.38 (3)	87 ± 5
K21-Cε	0.32 (3)	89 ± 45	0.49 (4)	135 ± 14
K23-Cε	0.47 (3)	101 ± 7	0.64 (2)	226 ± 19

Blank entries occur where no measurements were made. The carbon-proton distance was taken to be 0.109 nm in all cases. The uncertainties in S^2, the magnitudes of which are denoted by the numbers in parentheses for the last digit shown, and in τ_e are standard errors derived from the data fitting based upon the experimental uncertainties in Table 4. The χ^2 value listed is the sum of the squares of the fractional deviations of the calculated data from the experimental data normalized by the number of measurements.

Buckley, manuscript in preparation). The added flexibility that we notice beginning at G12 is obviously not due solely to the inherently greater flexibility expected at gly residues; G3, which is closer to an end of the peptide and which might be expected to be more mobile than a gly residue more "interior" (such as G12), actually has a higher order parameter. One obvious explanation from structural analysis of MLT is the absence of a hydrogen bond between T10 and P14, which could be responsible for the greater mobility of this segment of the peptide. Another possibility is that the segment from G12 onward (although we report only on G12–L16) might be less stabilized in the micelle relative to

the N-terminal portion and thus be less constrained by the lipid. This inference is consonant with the strongly cationic nature of the MLT carboxy-terminus.

By applying specific models of motion we can derive an estimate of the range of the angular excursions of the backbone C-H vectors, which would be consistent with the measured order parameters. For example, if they undergo restricted diffusion or a flag-waving motion (London and Avitabile, 1978; Kemple et al., 1994) about either the N-Cα bond or the Cα-carbonyl bond, an order parameter of ~0.7 yields an angular deviation of $\pm 40°$. Other models give similar results. Thus, even with the errors inherent in the measurements, the data strongly support the notion of a peptide backbone that is restricted in the mixed micelle, but nonetheless retains considerable mobility.

So far we have deduced features of mobility mainly from order parameters, but information on the nature of the internal motions is also available from τ_e values, which describe the apparent time scale of the motions. For the backbone Cα-H vectors the τ_e values were small (<90 ps) and in the NMR motional narrowing regime. The difference in τ_e for the same type of residue could be explained in terms of different segmental motions experienced by residues at different positions along the peptide chain; for example, at pH 7, τ_e is in the order G3 > G12, A4 > A15, L9 > L13 $\approx$ L16. The larger τ_e values occur for those residues that have larger order parameters.

N-terminus and side-chain dynamics

Compared with the highly flexible N-terminus of MLT in monomeric random coil and tetrameric α-helical conformations, which have order parameters of ~0.2 (P. Buckley, manuscript in preparation), the N-terminus mobility of MLT is more restricted in the mixed micelles (S^2 = 0.6–0.8). At pH 4 and 7 the restriction imposed on the internal motion of the MLT N-terminus most likely results from a general restriction in motion of the G1 to T11 portion of the MLT helix (see above) and from the electrostatic interaction between the phosphoryl moiety of the lipid headgroup and the cationic amino terminus. At pH 9 it seems likely that the deprotonated amino terminus might penetrate into the micelle, as noted earlier. However, any additional restriction on the backbone motion due to such penetration was not apparent in the order parameter values found for G1.

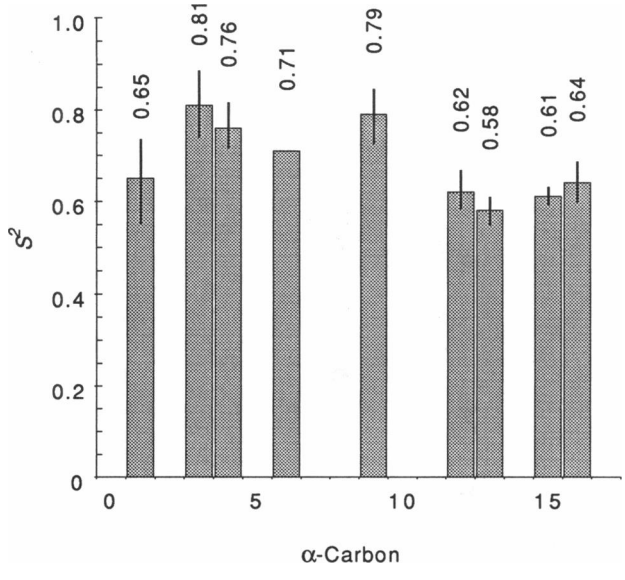

FIGURE 5 Histogram of the average of the order parameters for backbone Cα-H vectors of micelle-bound MLT at pH 4, 7, and 9. The standard deviations of the averages are indicated by the length of the solid lines at the top of each column.

The motions available to the C-H vectors of the trp indole moiety are mainly rotations about the χ_1 and χ_2 dihedral angles. Two ^{13}C labels were incorporated into the W19 indole ring, one at the δ_1 and the other at the ϵ_3 position, so that the indole motions could be characterized by two vectors with different orientations. As seen in Table 5, the order parameters of these two vectors are similar to those of the backbone Cα-H vectors, showing that the motion of the trp side chain is limited in the peptide-lipid mixed micelle, consistent with reports from fluorescence data (Bismuto et al., 1993; Chattopadhyay and Rukmini, 1993; John and Jähnig, 1988; Vogel and Rigler, 1987; Georghiou et al., 1982). (Weaver et al. (1992) reported a smaller order parameter for Cδ_1-W19 in micelle-bound MLT (~0.5). The reason for this apparent disagreement with the order parameter found here is that they made T_1 and NOE measurements at only one frequency. As a result, they were forced to make approximations in the data analysis that led to the choice of a different solution for S^2 and τ_e.) Based on the orientations of the Cδ_1-H and Cϵ_3-H vectors within the indole, the former vector should be more sensitive to rotation about the β-γ bond and the latter to rotation about the α-β bond. Because S^2 is larger for the Cδ_1-H vector than for the Cϵ_3-H vector, it becomes clear that the motion cannot be accounted for solely by rotation about the β-γ bond. Similar results were found for the trp residues in thioredoxin (Kemple et al., 1994). Although the internal motion of the trp moiety is complex, some notion of its angular extent can be achieved, nonetheless, from the Kinosita model, in which the vector is assumed to move within a cone of half-angle α (Kinosita et al., 1977). Our data yield fairly small values of α for a side chain; namely, $30° \leq \alpha \leq 40°$.

Helical wheel projections of MLT indicate that the trp residue should be on the hydrophobic face of the amphiphilic α-helix and therefore would be oriented toward the micelle interior, although the ring dimensions are such that relatively deep penetration is unlikely. Evidence in support of this model has been provided in the structure study of MLT bound to perdeuterated DPC micelles by Inagaki et al. (1989), where slow exchange of the trp amide proton with solvent was observed, and from fluorescence emission spectral blue shifts, which attend MLT-lipid interactions (Georghiou et al., 1982). This disposition of the side chain should in fact restrict its

motion in the lipid. Furthermore, some restriction in the motion might be attributable to hydrogen bonding between the indole ring of the trp and interfacial water molecules or neighboring lipid carbonyls, as suggested by Chattopadhyay and Rukmini (1993).

Fig. 6 shows the pH dependence of the order parameters for the lys side chains of MLT bound to MMPC micelles at pH 4, 7, 9, and 11. The order parameters are in the order $S^2(K7) < S^2(K21) < S^2(K23)$, irrespective of pH. Using the same model as applied to the backbone above, we find angular ranges of $\pm 100°$, $\pm 70°$, and $\pm 55°$, corresponding to order parameters 0.20 (K7), 0.30 (K21), and 0.47 (K23), respectively. This difference in motional behavior among the lys side chains can probably be accounted for by different environments for each lysine side chain and by the effects of electrostatic interactions. Stanislawski and Rüterjans (1987) investigated the insertion of MLT, labeled with ^{13}C-methyl groups on the ϵ-amino side chains of K7, K21, and K23, into bilayers. Such modification changes the cationic character of the amino groups by transforming the primary amine into a secondary amine and by adding molecular bulk, the latter possibly affecting molecular packing. Nonetheless, their results are consistent with ours. In particular, they found that the side chain of K7 seemed to be more flexible than those of K21 and K23. Inagaki et al. (1989) showed that for MLT bound to DPC micelles, K7 is fully exposed to solvent, whereas both K21 and K23 are nominally on the hydrophobic side of the MLT helix and are therefore expected to be oriented at least partially toward the micelle interior. Our observation that the side chain of K7 is the least restricted in motion and that of K23 the most correlates well with this ordering of solvent exposure. Similarly, Terwilliger et al. (1982) proposed an orientation of MLT in a phosphatidylcholine bilayer such that the side chain of K23 would be mostly buried in the bilayer, but with the end of its aliphatic chain (the ζ-NH_2 moiety) recurved to lie adjacent to the headgroups of the phospholipid; K21 was proposed to be at the bilayer-water interface. These authors assumed always, however, that the α-NH_2 of G1 was uncharged. Overall this model is supported by the data we have presented, particularly the order parameters, except that at both pH 4 and pH 7 all of the amino groups are cationic and none is therefore likely to penetrate into the interior of the micelle.

In general, larger τ_e values were observed for the lys and trp side chains, and the N-terminus, than for the backbone, apart from isolated exceptions (Table 5). It is interesting that these observations were made for two side chains that are presumed to be much differently disposed in the lipid, lys being exposed to solvent and trp not. The results for the apparent mobility of the lysyl side chains are thus somewhat counterintuitive and raise two obvious questions. First, are the τ_e values reliable? Second, if they are at least reasonably reliable, what do they mean and can we rationalize longer τ_e values for inherently flexible solvent exposed side chains than for the peptide main chain? Correlation times for the local motion are infrequently discussed, probably because of the difficulty of validating their accuracy and hence their reliability. It is for this reason that, where possible, we have compared values from NMR and fluorescence anisotropy decay data (Kemple et al., 1994, and see below). Nevertheless, in this study the consistent pattern in the τ_e values for the lysyl side chains is encouraging. The motions of the ultimate carbon atom in the lysine side chain are unavoidably sensitive to the hydration of the cationic nitrogen, to packing around the aliphatic portion of the side chain,

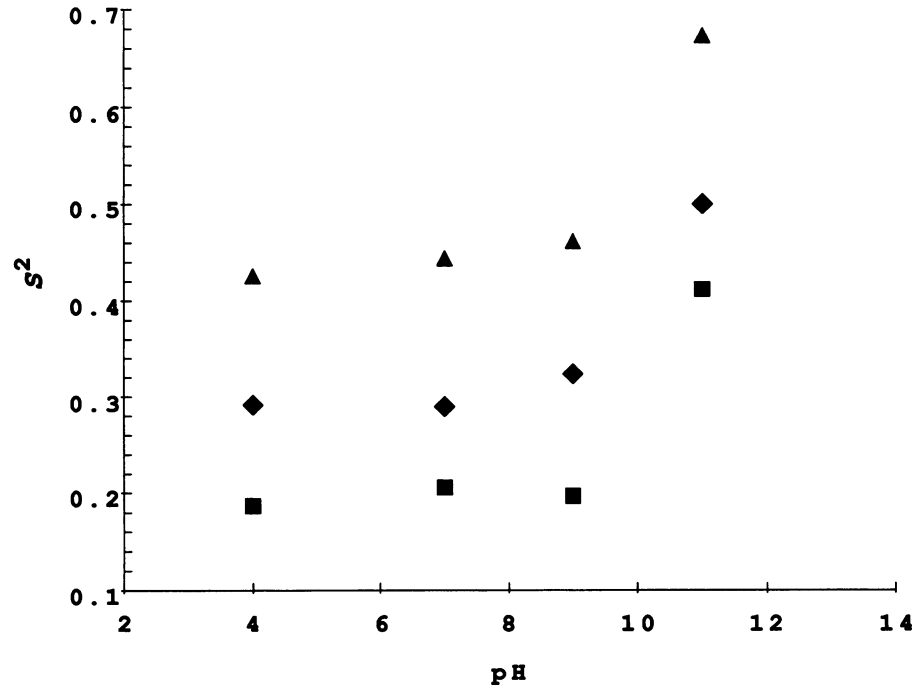

FIGURE 6 pH dependence of the order parameters of the lysine side-chain Cε-H vectors of micelle-bound MLT for K7 ■, for K21 ◆, and for K23 ▲.

somewhat to the dynamics of the lipid headgroups through electrostatic interactions, and to the viscosity of the solvent. For these reasons the longer τ_e values observed for the lys-Cϵ positions compared with the backbone positions seem sensible a priori.

However, there are other important considerations. The recovery of τ_e values on the order of 100 ps in no way negates the existence of even faster motions. In the Lipari and Szabo formalism τ_e is a weighted average of a collection of correlation times describing the internal motion in the entire side chain; thus τ_e would tend to be dominated by the longer times in the set. A correlation of S^2 and τ_e values within the trp and lys side chains similar to that seen in the backbone also was apparent, that is, larger τ_e values were associated with larger S^2. For trp in particular, S^2 and τ_e were substantially greater for the Cδ_1-H vector than for the Cϵ_3-H vector. (It is pertinent that the differences between τ_e values for the two different isotopically enriched trp residues generally did not appear in MLT monomer or tetramer dynamics (P. Buckley, manuscript in preparation).) This follows because T_1 (ϵ_3) > T_1 (δ_1) and NOE(δ_1) > NOE(ϵ_3). In a simple model of internal motion defined by only a single correlation time, one would expect identical τ_e values for two different vectors in the indole ring, provided the ring itself was effectively rigid. It is highly feasible, however, that different vectors in the indole moiety could have different τ_e values when complicated motions involving the χ_1 and χ_2 dihedral angles are occurring, because the weighting factors relating τ_e to the actual internal correlation times present should be different for different vectors, depending on the specific motions. In this case, the Cδ_1-H vector is more sensitive to slower internal motions than is the Cϵ_3-H vector. Given the degrees of freedom in the lysyl side chains, an even more complicated picture is likely.

Importantly, from time-resolved anisotropy measurements of W19 in a sample consisting of 70 μM MLT, 2.8 mM MMPC micelles in 50 mM phosphate at pH 7 in H_2O at 20°C, we found τ_m = 7.0 ns, S^2 = 0.68, τ_e = 77 ps, and r_o = 0.24, with standard errors on the order of 10%, where r_o is the initial anisotropy. S^2 and τ_e agree reasonably well with the NMR results for trp, and τ_m from fluorescence is just beyond the lower limit derived from the NMR data. (Even though solvent conditions were not the same for the fluorescence and NMR measurements, the viscosity of the solutions is similar, the lower temperature in the fluorescence measurements being compensated for by the use of D_2O in NMR.) We have observed such differences in τ_m values previously Kemple et al. (1994), and their origins remain to be determined.

Dynamics of the micelles

From first principles it seems inevitable in a mixed micelle that whereas the lipid would affect peptide mobility, the reverse should be true as well. Accordingly, to gain a better understanding of intrinsic lipid mobility, we also measured the ^{13}C relaxation parameters from natural abundance ^{13}C NMR of the MMPC itself in micellar form (40 mM MMPC, 50 mM phosphate at pH 7 and 25°C; data not shown). Individual signals from the glycerol backbone, from the choline group, and from the first three carbons at the top of the acyl chain and the last three at the bottom were resolved, whereas the eight methylene carbons near the center of the acyl chain gave only a single signal. In general, going from the omega end of the acyl chain, the order parameters increased from ~0.01 to ~0.2, which is similar to results found in other micellar systems (Söderman et al., 1985). The largest order parameters were found for the glycerol backbone (~0.5) and the smallest overall for the terminal methyls on the choline group and the acyl chain (~0.01). This result is in keeping with the highly fluid lipidic core. In mixed micelles with MLT at a lipid-to-peptide ratio of 40:1, the order parameters increased for the two aliphatic carbons near the top of the acyl chain to ~0.3 (carbons 12 and 13 counting from the omega end), and the glycerol backbone order parameters showed a slight increase. Note that these represent average effects of the MLT, because clearly not every lipid molecule interacts directly with MLT. The τ_m values, 14 ± 2 ns both with and without MLT, were somewhat larger than τ_m found from the MLT relaxation measurements but agreed within the experimental uncertainties. These results show that even though the binding of MLT did not yield detectable changes in lipid ^{13}C chemical shifts (described earlier), effects were manifested in changes in lipid dynamics. The clearer influence of MLT binding on the lipid headgroup was expected, as were the (albeit small) changes seen in acyl chain dynamics.

pH 11 results

At pH 11 there were indications that the MLT-micelle interactions were altered, even though the MLT Cα chemical shifts remained consistent, with a mainly helical conformation of residues 1–16 (Table 2). In particular, deeper penetration of MLT into the interior of the micelle, changes in the orientation of the MLT helix relative to the acyl chains, and/or changes in the mixed micelles themselves appear to occur at pH 11, as suggested by i) the observation of generally broader ^{13}C-NMR lines from MLT at pH 11 relative to pH 4; e.g., G3α: 66.7 Hz vs. 40.9 Hz; A15α: 58.9 Hz vs. 36.2 Hz; L13α: 64.0 Hz vs. 26.7 Hz; K23ϵ: 48.3 Hz vs. 22.0 Hz; ii) the disappearance of interaction of MLT with the MMPC headgroups (see below); iii) an increase in τ_m (Table 5); and iv) increased restriction of the local motion of the lys side chains (Table 5 and Fig. 6). A change in orientation at pH 11 could be explained by the elimination of positive charges on the side chains of K7, K21, and K23, which all have pK_a values in the micelle complexes of around 10.5 (Zhu et al., 1995b). (The changes in the chemical shifts of the $^{13}C\epsilon$ resonances of the three lysine residues at pH 11 are almost certainly due to

deprotonation of their ε-amino groups and not to conformational effects.) Thus, at pH 11 only two positive charges would remain on MLT, namely those of R22 and R24 near the C-terminus, allowing the uncharged segment comprising residues 1 to 21 (or part thereof) to penetrate more deeply into the hydrophobic core of the micelle. Thereafter, conformational exchange and the slower overall tumbling rate could account for the ^{13}C-NMR line broadening.

An intriguing observation is that at pH 11 the interaction between MLT and the MMPC headgroup was not detected in the ^{31}P experiments ($\Delta\nu_{mmpc\text{-}mlt} \approx 0$, Table 3, Fig. 5), even though the arg side chains are still positively charged. It has been pointed out that the two arg residues contribute little to the total interfacial charge of MLT when MLT binds with membranes (Stankowski and Schwarz, 1990; de Kroon et al., 1991). The interpretation given by Stankowski and Schwarz is that the arg side chains either are positioned farther from the membrane-water interface than the lys side chains, or they are tightly associated with counter-ions. However, the former is inconsistent with the situation encountered in detergent micelles, as pointed out by Stankowski and Schwarz (1990), where the various charged groups of MLT are found at approximately equal distances from the interface (Brown et al., 1982). As noted above, the interaction of phosphate with a guanidinium group is promoted by the formation of a ring structure, so it is feasible that phosphate bound to MLT would hinder the interaction of the phosphoryl group of MMPC with the arg guanidinium groups. There is yet a third possible explanation, namely, that the guanidinium cations and the phosphoryl moieties of the lysolipid cannot orient properly for optimal interaction. In any event, the lack of a detectable interaction of MLT with the MMPC headgroups at pH 11 is not inconsistent with the constant charge of MLT sensed by the MMPC micelle at lower pH.

CONCLUSIONS

The following conclusions are evident from this work.

1. MLT becomes predominantly α-helical upon binding to MMPC micelles. The helical transformation is clear, even at low lipid-to-peptide ratios (1:2), and is probably initiated by hydrophobic interactions. The precise form of the mixed micelle is very likely dependent on the lipid-to-peptide ratio; stable, well-defined micelles are formed only at molar ratios of ≥30:1. Under all conditions the exchange between free and bound MLT is slow. At lipid-to-peptide ratios below 4:1 the exchange rate was found to lie in the range of 200–425 s^{-1}.

2. The MLT α-helix (at least involving residues 1–16) in the MLT-MMPC mixed micelle is stable in the pH range 4 to 11. Hexacationic MLT as well as dicationic MLT (at pH 11) bind in a stable fashion to MMPC, implying that neither the α-amino nor the ζ-amino moieties (of lys) must be deprotonated for lipid binding to occur.

3. ^{31}P-NMR linewidth analysis indicates that phosphate ions "bind" to MLT in the complexes predominantly at the N-terminus, at one or more of the three lysine side chains, and at the two arginine side chains.

4. The cationic groups of MLT in the micelle are exposed to solvent from pH 4 to pH 7; the extent decreases gradually from pH 7 to pH 11. This reduction is probably effected by deprotonation of the NH_2 groups of the amino terminus and the lysine side chains at high pH. Such changes in the total cationic charge and its distribution probably promote a change in position and orientation of the MLT helix in the micelle.

5. A constant positive charge on the peptide is sensed by the MMPC headgroup up to pH 10 but is reduced to nearly zero at pH 11. This implies that the charges on the two arginine side chains do not significantly contribute to the interaction of MLT with the MMPC headgroups, consistent with published work (e.g., Stankowski and Schwarz, 1990).

6. The backbone and side chains of MLT in the mixed micelle are partially, but certainly not completely, immobilized. Order parameters are ~0.5–0.8 for the backbone α-carbons, ~0.6–0.8 for the trp side chain, and ~0.2–0.5 for the lys side chains, and they showed no obvious dependence on pH in the range 4 to 9.

7. The amino-terminal gly residue, which rotates nearly freely in monomeric MLT, is restricted in mobility in the mixed micelle, its amplitude of motion becoming essentially equivalent to that of the backbone Cα-H moieties. In other words, lipid binding eliminates "end effects" on MLT mobility. The partial immobilization of G1 may depend on both electrostatic interactions, because the immobilization is evident at pH 4, where the residue is charged, and on packing of lipid molecules around the residue, because the order parameter for G1 is nearly the same at pH 9, where it is not charged.

8. The motion of α-carbons in the N-terminal part (residues 3–9) of MLT is more rigidly constrained than that of α-carbons in the C-terminal part (13–16). This is reasonable because the hydrophobic residues in the N-terminal half of MLT provide better anchoring into the lipid milieu and because there are competing electrostatic interactions between the cationic C-terminal end of MLT and the zwitterionic phosphatidylcholine moieties.

9. The motion of the indole moiety of W19 is fairly restricted, consistent with a location amid the fatty acyl moieties in the mixed micelle. The side chains of K7 and K21 are highly mobile in the mixed micelle; the side chain of K23 is likewise quite mobile, although somewhat less so than K7 and K21, and is not immobilized at any pH. This implies that the amino group of lys-23 in charged or uncharged form is not buried in the hydrophobic core of the micelle, although it is possible that the aliphatic portion of the side chain could be looped to interact partially with the acyl chains.

10. Generally τ_e values seem to fall into two groups. The large majority of the backbone α-carbons have τ_e values < 50 ps, whereas side-chain τ_e values lie between 50 and 120 ps at pH values 4–9. As noted, the lysyl side chains are

charged and solvated in the MLT-MMPC mixed micelle (at pH < 10); only the indole of W19 is apparently partially buried in the micellar "interior." The relatively longer correlation time for the trp side chain probably derives from collective indole-lipid acyl chain motions promoted by van der Waal's interactions.

11. At pH 11, τ_m is larger than at pH 4 (16 ns versus 10 ns), and the order parameters of the lys residues were also markedly larger, the latter indicating that the then uncharged lysine residues are more likely to penetrate into the lipid.

12. Although lipid packing (both headgroup and acyl chain) is substantially greater in lipid bilayers formed from fully acylated phospholipids than in micelles comprising lysophospholipids, we believe the nature of interaction with MLT will be essentially the same for both lipid systems. It seems likely a priori that the tightness of the binding and the amplitudes and rate of backbone and side-chain dynamics for bound MLT will depend on the thermotropic phase of the lipid bilayer being studied and on the net charge in the bilayer.

We thank Dr. Paul Buckley for assisting in preparation of some of the peptides and for the program used in analyzing the relaxation data; Dr. Noberto Silva for measuring $r(t)$; Dr. B. D. Ray of the IUPUI NMR Center for maintenance and smooth operation of the NMR spectrometers; and Ms. Lingyang Zhu for assisting in data analysis.

This work was supported in part by NSF grant DMB-9105885 to MDK and by PHS grant GM34847 to FGP.

REFERENCES

Abragam, A. 1961. Thermal relaxation in liquids and gases. *In* Principles of Nuclear Magnetism. Clarendon Press, Oxford. 264–353.

Altenbach, C., and W. L. Hubbell. 1988. The aggregation state of spin-labeled melittin in solution and bound to phospholipid membranes: evidence that membrane-bound melittin is monomeric. *Proteins Struct. Funct. Genet.* 3:230–242.

Anderson, D., T. C. Terwilliger, W. Wickner, and D. Eisenberg, 1980. Melittin forms crystals which are suitable for high resolution x-ray structural analysis and which reveals a molecular 2-fold axis of symmetry. *J. Biol. Chem.* 255:2578–2582.

Bangham, A. D., and R. C. Dawson. 1959. The relation between the activity of a lecithinase and the electrophoretic charge of the substrate. *Biochem. J.* 72:486–492.

Barbato, G., M. Ikura, L. E. Kay, R. W. Pastor, and A. Bax. 1992. Backbone dynamics of calmodulin studied by ^{15}N relaxation using inverse detected two-dimensional NMR spectroscopy: the central helix is flexible. *Biochemistry.* 31:5269–5278.

Bazzo, R., M. J. Tappin, A. Pastore, T. S. Harvey, J. A. Carver, and I. D. Campbell. 1988. The structure of melittin: a ^1H-NMR study in methanol. *Eur. J. Biochem.* 173:139–146.

Bello, J., H. R. Bello, and E. Granados. 1982. Conformation and aggregation of melittin: dependence on pH and concentration. *Biochemistry.* 21:461–465.

Bernheimer, A. W., and B. Rudy. 1986. Interactions between membranes and cytolytic peptides. *Biochim. Biophys. Acta.* 864:123–141.

Beschiaschvili, G., and J. Seelig. 1990. Melittin binding to mixed phosphatidylglycerol/phosphatidylcholine membranes. *Biochemistry.* 29:52–58.

Bismuto, E., I. Sirangelo, and G. Irace. 1993. Folding and dynamics of melittin in reversed micelles. *Biochim. Biophys. Acta.* 1146:213–218.

Boyd, J., U. Hommel, and I. D. Campbell. 1990. Influence of cross-correlation between dipolar and anisotropic chemical shift relaxation mechanisms upon longitudinal relaxation rates of ^{15}N in macromolecules. *Chem. Phys. Lett.* 175:477–482.

Brauner, J. W., R. Mendelsohn, and F. G. Prendergast. 1987. Attenuated total reflectance fourier transform infrared studies of the interaction of melittin, two fragments of melittin and d-hemolysin with phosphatidylcholines. *Biochemistry.* 26:8151–8158.

Brown, L. R., W. Braun, A. Kumar, and K. Wüthrich. 1982. High-resolution nuclear magnetic resonance studies of the conformation and orientation of melittin bound to a lipid-water interface. *Biophys. J.* 37:319–328.

Brown, L. R., J. Lauterwein, and K. Wüthrich. 1980. High-resolution ^1H-NMR studies of self-aggregation of melittin in aqueous solution. *Biochim. Biophys. Acta.* 622:231–244.

Buckley, P., A. S. Edison, M. D. Kemple, and F. G. Prendergast. 1993. $^{13}C^{\alpha}$-NMR assignments of melittin in methanol and chemical shift correlations with secondary structure. *J. Biomol. NMR.* 3:639–652.

Chattopadhyay, A., and R. Rukmini. 1993. Restricted mobility of the sole tryptophan in membrane-bound melittin. *FEBS Lett.* 335:341–344.

Dawson, C. R., A. F. Drake, J. Helliwell, and R. C. Hider. 1978. The interaction of bee melittin with lipid bilayer membranes. *Biochim. Biophys. Acta.* 510:75–86.

de Kroon, A. I. P. M., J. A. Killian, J. de Gier, and B. de Kruijff. 1991. The membrane interaction of amphiphilic model peptides affects phosphatidylserine headgroup and acyl chain order and dynamics. Application of the "phospholipid headgroup electrometer" concept to phosphatidylserine. *Biochemistry.* 30:1155–1162.

Dempsey, C. E. 1990. The actions of melittin on membranes. *Biochim. Biophys. Acta.* 1031:143–161.

Dempsey, C. E., M. Bitbol, and A. Watts. 1989. Interaction of melittin with mixed phospholipid membranes composed of dimyristoylphosphatidylcholine and dimyristoylphosphatidylserine studied by deuterium NMR. *Biochemistry.* 28:6950–6956.

Dempsey, C. E., and G. S. Butler. 1992. Helical structure and orientation of melittin in dispersed phospholipid membranes from amide exchange analysis in situ. *Biochemistry.* 31:11973–11977.

Drake, A. F., and R. C. Hider. 1979. The structure of melittin in lipid bilayer membranes. *Biochim. Biophys. Acta.* 555:371–373.

Duncan, T. M. 1990. A Compilation of Chemical Shift Anisotropy. Farragut Press, Chicago. C-4.

Faucon, J. F., J. Dufourcq, and C. Lussan. 1979. The self-association of melittin and its binding to lipids. *FEBS Lett.* 102:187–190.

Fischgold, H., and E. Chain. 1934. The spontaneous decomposition of lecithin and its bearing on the determination of the isoelectric point. *Biochem. J.* 28:2044–2051.

Frey, S., and L. K. Tamm. 1991. Orientation of melittin in phospholipid bilayers: a polarized attenuated total reflection infrared study. *Biophys. J.* 60:922–930.

Georghiou, S., M. Thompson, and A. K. Mukhopadhyay. 1982. Nature of melittin-phospholipid interaction. *Biophys. J.* 37:159–160.

Gierasch, L. M., J. E. Lacy, K. F. Thompson, A. L. Rockwell, and P. I. Watnick. 1982. Conformations of model peptides in membrane-mimetic environments. *Biophys. J.* 37:275–284.

Goto, Y., and Y. Hagihara. 1992. Mechanism of the conformational transition of melittin. *Biochemistry.* 31:732–738.

Haberkorn, R. A., R. E. Stark, H. van Willigen, and R. G. Griffin. 1981. Determination of bond distances and bond angles by solid-state nuclear magnetic resonance. ^{13}C and ^{14}N NMR study of glycine. *J. Am. Chem. Soc.* 103:2534–2539.

Habermann, E. 1972. Bee and wasp venoms. *Science.* 177:314–322.

Habermann, E., and J. Jentsch. 1967. Sequenzanalyse des melittins aus den tryptischen und peptischen Spaltstücken. *Z. Physiol. Chem.* 348:37–50.

Hauser, H., M. C. Phillips, B. A. Levine, and R. J. Williams. 1975. Ion-binding to phospholipids. Interaction of calcium and lanthanide ions with phosphatidylcholine (lecithin). *Eur. J. Biochem.* 58:133–144.

Ichimura, S., K. Mita, and M. Zama. 1978. Conformation of poly (L-arginine). I. Effects of anions. *Biopolymers.* 17:2769–2782.

Ikura, T., N. Gô, and F. Inagaki. 1991. Refined structure of melittin bound to perdeuterated dodecylphosphocholine micelles as studied by two-dimensional NMR and distance geometry calculations. *Proteins Struct. Funct. Genet.* 9:81–89.

Inagaki, F., I. Shimada, K. Kawaguchi, M. Hirano, I. Terasawa, T. Ikura, and N. Gô. 1989. Structure of melittin bound to perdeuterated dode-

cylphosphocholine micelles as studied by two-dimensional NMR and distance geometry calculations. *Biochemistry.* 28:5985–5991.

John, E., and F. Jähnig. 1988. Dynamics of melittin in water and membranes as determined by fluorescence anisotropy decay. *Biophys. J.* 54:817–827.

John, E., and F. Jähnig. 1991. Aggregation state of melittin in lipid vesicle membranes. *Biophys. J.* 60:319–328.

Kemple, M. D., P. Yuan, K. E. Nollet, J. A. Fuchs, N. Silva, and F. G. Prendergast. 1994. ^{13}C NMR and fluorescence analysis of tryptophan dynamics in wild-type and two single-trp variants of *Escherichia coli* thioredoxin. *Biophys. J.* 66:2111–2126.

Kinosita, K. S., S. Kawato, and A. Ikegami. 1977. A theory of fluorescence polarization decay in membranes. *Biophys. J.* 20:289–305.

Knöppel, E., D. Eisenberg, and W. Wickner. 1979. Interactions of melittin, a preprotein model, with detergents. *Biochemistry.* 18:4177–4181.

Kreil, G., C. Mollay, R. Kaschnitz, L. Haiml, and U. Vilas. 1980. Prepromelittin: specific cleavage of the pre- and the propeptide in vitro. *Ann. N.Y. Acad. Sci.* 343:338–346.

Kuchinka, E., and J. Seelig. 1989. Interaction of melittin with phosphatidylcholine membranes. Binding isotherm and lipid-head-group conformation. *Biochemistry.* 28:4216–4221.

Lauterwein, J. L., C. Bösch, L. R. Brown, and K. Wüthrich. 1979. Physiochemical studies of the protein-ligand interactions in melittin-containing micelles. *Biochim. Biophys. Acta.* 556:244–264.

Lauterwein, J. L., R. Brown, and K. Wüthrich. 1980. High-resolution ^{1}H-NMR studies of monomeric melittin in aqueous solution. *Biochim. Biophys. Acta.* 622:219–230.

Lipari, G., and A. Szabo. 1982. Model-free approach to the interpretation of nuclear magnetic resonance relaxation in macromolecules. 1. Theory and range of validity. *J. Am. Chem. Soc.* 104:4546–4559.

London, R. E., and J. Avitabile. 1978. Calculated ^{13}C relaxation parameters for a restricted internal diffusion model. Application to methionine relaxation in dihydrofolate reductase. *J. Am. Chem. Soc.* 100: 7159–7165.

Mackler, B. F., and G. Kreil. 1977. Honey bee venom melittin. Correlation of nonspecific inflammatory activities with amino acid sequences. *Inflammation.* 2:55–65.

Mandel, A. M., M. Akke, and A. G. Palmer, III. 1995. Backbone dynamics of *Escherichia coli* ribonuclease HI: correlations with structure and function in an active enzyme. *J. Mol. Biol.* 246:144–163.

Martin, M. L., J.-J. Delpeuch, and G. J. Martin. 1980. Relaxation time determination. *In* Practical NMR Spectroscopy. Heyden and Sons, London. 244–290.

Naito, A., S. Ganapathy, K. Alasaka, and C. A. McDowell. 1981. Chemical shielding tensor and ^{13}C-^{14}N dipolar splitting in single crystals of L-alanine. *J. Chem. Phys.* 74:3190–3197.

Plückthun, A., and E. A. Dennis. 1982. Acyl and phosphoryl migration in lysophospholipids: importance in phospholipid synthesis and phospholipase specificity. *Biochemistry.* 21:1743–1750.

Podo, F., R. Strom, C. Crifò, and M. Zulauf. 1982. Dependence of melittin structure on its interaction with multivalent anions and with model membrane systems *Int. J. Pept. Protein Res.* 19:514–527.

Quay, S. C., and C. C. Condie. 1983. Conformational studies of aqueous melittin: thermodynamic parameters of the monomer-tetramer self-association reaction. *Biochemistry.* 22:695–700.

Reily, M. D., T. Venkataraman, and D. O. Omencinsky. 1992. Structure-induced carbon-13 chemical shifts: a sensitive measure of transient localized secondary structure in peptides. *J. Am. Chem. Soc.* 114: 6251–6252.

Rifkind, J. M., and G. L. Eichhorn. 1970. Specificity for the interaction of nucleotides with basic polypeptides. *Biochemistry.* 9:1753–1761.

Roux, M., J-M. Neuman, R. S. Hodges, P. F. Deveaux, and M. Bloom. 1989. Conformational changes of phospholipid headgroups induced by a cationic integral membrane peptide as seen by deuterium magnetic resonance. *Biochemistry.* 29:2313–2321.

Schwartz, G., and G. Beschiaschvili. 1988. Kinetics of melittin self-association in aqueous solution. *Biochemistry.* 27:7826–7831.

Schwartz, G., and G. Beschiaschvili. 1989. Thermodynamic and kinetic studies on the association of melittin with a phospholipid bilayer. *Biochim. Biophys. Acta.* 979:82–90.

Separovic, F., K. Hayamizu, R. Smith, and B. A. Cornell. 1991. C-13 chemical shift tensor of L-tryptophan and its application to peptide structure determination. *Chem. Phys. Lett.* 181:157–162.

Smith, R., F. Separovic, T. J. Milne, A. Whittaker, F. M. Bennett, B. A. Cornell, and A. Makriyannis. 1994. Structure and orientation of the pore-forming peptide, melittin, in lipid bilayers. *J. Mol. Biol.* 241:456–466.

Söderman, O., H. Walderhaug, U. Henriksson, and P. Stilbs. 1985. NMR relaxation in isotropic surfactant systems. *A* ^{2}H, ^{13}C, and ^{14}N, NMR study of the micellar (L_1) and cubic (I_1) phases in the dodecyltrimethylammonium chloride/water system. *J. Phys. Chem.* 89:3693–3701.

Spera, S., and A. Bax. 1991. Empirical correlation between protein backbone conformation and Cα and Cβ ^{13}C nuclear magnetic resonance chemical shifts. *J. Am. Chem. Soc.* 113:5490–5492.

Stafford, R. E., T. Fanni, and E. A. Dennis. 1989. Interfacial properties and critical micelle concentration of lysophospholipids. *Biochemistry.* 28: 5113–5120.

Stanislawski, R., and H. Rüterjans. 1987. C-NMR investigation of the insertion of bee venom melittin into lecithin vesicles. *Eur. Biophys. J.* 15:1–12.

Stankowski, S., and G. Schwarz. 1990. Electrostatics of a peptide at a membrane/water interface. The pH dependence of melittin association with lipid vesicles. *Biochim. Biophys. Acta.* 1025:164–172.

Strom, R., C. Crifo, V. Viti, L. Guidoni, and F. Podo. 1980. On the structure of melittin in aqueous solutions and upon interaction with membrane model systems. *In* Developments in Biophysical Research. A. Borsellino, editor. Plenum Press, New York. 117–130.

Talbot, J. C., J. Dufourcq, J. de Bony, J. Faucon, and C. Lussan. 1979. Conformational changes and self association of monomeric melittin. *FEBS Lett.* 102:191–193.

Terwilliger, T. C., and D. Eisenberg. 1982a. The structure of melittin. I. Structure determination and partial refinement. *J. Biol. Chem.* 257: 6010–6015.

Terwilliger, T. C., and D. Eisenberg. 1982b. The structure of melittin. II. Interpretation of the structure. *J. Biol. Chem.* 257:6016–6022.

Terwilliger, T. C., L. Weissman, and D. Eisenberg. 1982. The structure of melittin in the form I crystals and its implication for melittin's lytic and surface activity. *Biophys. J.* 37:353–361.

Vogel, H. 1987. Comparison of the conformation and orientation of alamethicin and melittin in lipid membranes. *Biochemistry.* 26: 4562–4572.

Vogel, H., and F. Jähnig. 1986. The structure of melittin in membranes. *Biophys. J.* 50:573–582.

Vogel, H., and R. Rigler. 1987. Orientational fluctuations of melittin in lipid membranes as detected by time-resolved fluorescence anisotropy measurements. *In* Structure, Dynamics and Function of Biomolecules. A. Ehrenberg, R. Rigler, L. Nilsson, and G. J. Gräslund, editors. Springer, Berlin. 289–294.

Weast, R. C. 1983. CRC Handbook of Chemistry and Physics. Chemical Rubber Co., Boca Raton, FL.

Weaver, A. J., M. D. Kemple, J. W. Brauner, R. Mendelsohn, and F. G. Prendergast. 1992. Fluorescence, CD, attenuated total reflectance (ATR) FTIR, and ^{13}C NMR characterization of the structure and dynamics of synthetic melittin and melittin analogues in lipid environments. *Biochemistry.* 31:1301–1313.

Wilcox, W., and D. Eisenberg. 1992. Thermodynamics of melittin tetramerization determined by circular dichroism and implications for protein folding. *Protein Sci.* 1:641–653.

Wishart, D. S., C. G. Bigam, A. Holm, R. S. Hodges, B. D. Sykes, and F. M. Richards. 1995. ^{1}H, ^{13}C and ^{15}N random coil NMR chemical shifts of the common amino acids. I. Investigations of nearest-neighbor effects. *J. Biomol. NMR.* 5:67–81.

Wishart, D. S., B. D. Sykes, and F. M. Richards. 1991. Relationship between nuclear magnetic resonance chemical shift and protein secondary structure. *J. Mol. Biol.* 222:311–333.

Zhu, L., M. D. Kemple, S. B. Landy, and P. Buckley. 1995a. Effect of dipolar cross correlation on model-free motional parameters obtained from ^{13}C relaxation in AX_2 systems. *J. Magn. Reson. B.* 109:19–30.

Zhu, L., M. D. Kemple, P. Yuan, and F. G. Prendergast. 1995b. N-terminus and lysine side chain pK_a values of melittin in aqueous solution and micellar dispersions measured by ^{15}N NMR. *Biochemistry.* 34: 13196–13202.